Radio-frequency evaporation in an optical dipole trap

Raphael Lopes
Laboratoire Kastler Brossel, Collège de France, CNRS,
ENS-PSL Research University, Sorbonne Université, 11 place Marcelin Berthelot, 75005 Paris, France

(Received 8 April 2021; revised 9 July 2021; accepted 30 July 2021; published 10 September 2021)

We present an evaporative cooling technique for atoms trapped in an optical dipole trap that benefits from narrow optical transitions. For an appropriate choice of wavelength and polarization, a single laser beam leads to opposite light shifts in two internal states of the lowest-energy manifold. Radio-frequency coupling between these two states results in evaporative cooling at a constant trap stiffness. The evaporation protocol is well adapted to several atomic species, in particular to the case of Lanthanides such as Er, Dy, and fermionic Yb, but also to alkali-earth metals such as fermionic Sr. We derive the dimensionless expressions that allow us to estimate the evaporation efficiency. As a concrete example, we consider the case of ^{162}Dy and present a numerical analysis of the evaporation in a dipole trap near the $J' = J$ optical transition at 832 nm. We show that this technique can lead to runaway evaporation in a minimalist experimental setup.

DOI: 10.1103/PhysRevA.104.033313

I. INTRODUCTION

A key step to achieve Bose-Einstein condensation [1] is the evaporative cooling technique introduced in the 1990s [2–5]. Such a mechanism is qualitatively simple to understand; particles with high energy, above a given cutoff energy, ϵ_c, are lost from the system followed by subsequent thermalization. The truncated Boltzmann distribution readjusts, and the temperature falls at the cost of particle loss.

This process has proved successful in cold atom experiments, in both magnetic and optical traps [6–10]. In magnetic traps, a magnetic field gradient ensures that atoms prepared in a low-field seeking internal state are trapped while atoms in a high-field seeking state are expelled. The coupling between the two states is ensured by a radio-frequency (RF) photon, whose frequency is progressively swept to reduce the cutoff energy. For efficient evaporative cooling to occur the elastic collision rate, $\Gamma_{\text{el.}}$, needs to dominate over the loss rate, Γ_{loss}. In that case, evaporative cooling accelerates over time, reaching degeneracy at the cost of minimal particle loss.

Nowadays, most cold atom experiments use evaporative cooling in optical dipole traps as it allows the cooling of different internal states and species with zero magnetic moment [11–16]. However, it comes at the cost of reduced evaporation efficiency, as the evaporation is performed by continuously decreasing the trap depth, which softens the potential and reduces the elastic collision rate [17]. More elaborated strategies, such as addressing resonant optical transitions [18], combining dipole traps with very different volumes [19–21], or changing the s-wave scattering length, a, [15] during the evaporation, allow us to mitigate this issue but lead to an enhanced experimental complexity and secondary inelastic processes [22].

Here, we propose to cool a sample trapped in a single Gaussian laser beam, with wavelength λ_L, close to a narrow optical transition λ_1 (see Fig. 1). The two lowest-energy states, $|d\rangle$ and $|b\rangle$, can, for a given polarization, feel opposite light shifts. For instance, if $|d\rangle$ is not coupled to $|e_1\rangle$ (see Fig. 1), its polarizability is set by other far-detuned excited states, that we regroup under $|e_2\rangle$, from which the laser beam is detuned by Δ, with $|\Delta| \gg \delta$. On the other hand, the polarizability of the bright state $|b\rangle$ is, to a good approximation, simply defined by the detuning from the narrow optical transition, δ, and the transition linewidth Γ. For $\delta > 0$, $|b\rangle$ has a negative polarizability and therefore the atoms feel a repulsive potential at the intensity maximum, while atoms in $|d\rangle$ are trapped for $\Delta < 0$. Coupling the two internal states, for instance through radio frequency, results in evaporative cooling in an optical trap with a fixed trap stiffness, where ϵ_c is set by the radio frequency.

This technique is experimentally simple to implement as it only requires a single, tightly focused, laser beam overlapping with the atomic cloud. Several advantages of optical dipole traps are still applicable, such as the possibility to cool two distinct internal states, in the case of two dark states, sympathetic cooling of atomic mixtures, and evaporative cooling of states with zero magnetic moment. Moreover, the same protocol can be extended to boxlike potentials [23]. Compared to the cooling technique reported in Ref. [18], our method is experimentally less demanding as we do not require a long-lived metastable state nor antimagic wavelengths.

II. APPLICABILITY TO DIFFERENT ATOMIC SPECIES

In summary, two main ingredients are required to perform the discussed radio-frequency evaporation in an optical dipole trap: a ground manifold with a nonzero total spin and a narrow optical transition. Importantly, the narrowness of the optical transition ensures that atoms in $|b\rangle$ are not repumped into $|d\rangle$ before escaping the laser beam spatial profile. For that

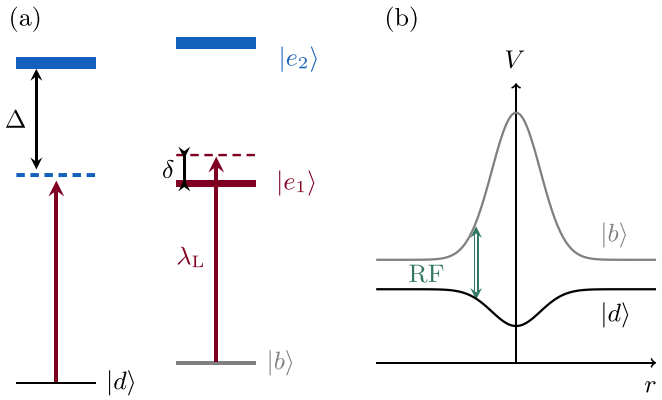

FIG. 1. Schematic representation of RF evaporation in an optical dipole trap. (a) Schematic energy representation of the two lowest-energy states $|d\rangle$ and $|b\rangle$, and excited states $|e_1\rangle$ and $|e_2\rangle$. A laser beam with wavelength λ_L induces opposite light shifts for the two states. (b) Spatial dependence of the optical potential for the dark state $|d\rangle$ and bright state $|b\rangle$ for $\Delta/\delta < 0$. Radio-frequency couples the two states and defines the cutoff energy for atoms in $|d\rangle$.

purpose, the incoherent photon scattering rate needs to be much smaller than the escaping rate, which translates, for $|\Delta| \gg \delta$, into the condition $\delta/\Gamma \gg \sqrt{U_b m w_0^2/\hbar^2}$, where $U_b = \hbar\Omega^2/\delta$ is the repulsive potential felt by atoms in $|b\rangle$, Ω the Rabi frequency, w_0 the laser beam radius at $1/e^2$, $\hbar$ the reduced Planck constant, and m the atomic mass.

Dysprosium and erbium atomic species verify both conditions, and are thus good candidates for the envisioned cooling protocol. In the case of dysprosium, an interesting choice is the $J' = J$ transition with wavelength $\lambda_1 \approx 832\,\text{nm}$, and linewidth $\Gamma \approx 2\pi \times 11\,\text{kHz}$. A similar transition exists for erbium around 847.5 nm [24]. Other species can also benefit from this evaporation protocol, such as fermionic strontium and ytterbium near the narrow optical transitions $F \to F' = F$ at 689 nm and 556 nm, respectively [16,25], or in the case of titanium, using the $J' = J = 4$ transition at 546 nm with linewidth $\Gamma \approx 2\pi \times 300\,\text{kHz}$ [26].

III. RATE EQUATIONS

In order to estimate the evaporation efficiency of this protocol we use the truncated Boltzmann distribution approximation developed in Ref. [3]. Using a constant value of $\eta = \epsilon_c/k_B T$, we write the instantaneous time variation of the atom number, N, total energy, E, and temperature, T,

$$\dot{N} = \dot{N}_{\text{ev.}} + \dot{N}_{\text{spl.}} + \dot{N}_{\text{loss}} \tag{1}$$

$$\dot{E} = \dot{E}_{\text{ev.}} + \dot{E}_{\text{spl.}} + \dot{E}_{\text{loss}} + \dot{E}_{\text{heat.}} \tag{2}$$

$$\dot{T}/T = \dot{E}/E - \dot{N}/N, \tag{3}$$

where $N_{\text{ev.}}$ and $E_{\text{ev.}}$ are associated to atom loss and energy reduction through evaporation, $N_{\text{spl.}}$ and $E_{\text{spl.}}$, to particle spilling from the trap, N_{loss} and E_{loss} one-body losses through collisions with the residual background gas, and $E_{\text{heat.}}$ heating induced by incoherent photon scattering processes (see below). The internal energy is given by $E = N k_B T \tilde{c}$, with $\tilde{c} = d \ln \xi / d \ln T$, and $\xi = (1/n\lambda^3) \int_0^\infty d\epsilon\, \rho(\epsilon) f(\epsilon)$, where

$$\rho(\epsilon) = \frac{2\pi (2m)^{3/2}}{(2\pi\hbar)^3} \int_{U(r)\leqslant\epsilon} d^3\mathbf{r} \sqrt{\epsilon - U(\mathbf{r})}, \tag{4}$$

is the energy density of states, $f(\epsilon) = n\lambda^3 e^{-\epsilon/k_B T}\Theta(\epsilon_c - \epsilon)$ the truncated Boltzmann distribution, $U(\mathbf{r})$ the conservative optical potential felt by atoms in d, n the density, λ the de-Broglie wavelength, k_B the Boltzmann constant, and $\Theta(\epsilon)$ the Heaviside step function.

Four processes define the evolution of temperature and atom number [3–5,27]. The loss of particles through evaporation leads to changes of atom number and total energy,

$$\dot{N}_{\text{ev.}}/N = -\Gamma_{\text{ev.}}\, n\sigma v \tag{5}$$

$$\dot{E}_{\text{ev.}}/E = -\frac{\Gamma_{\text{ev.}}}{\tilde{c}} \tilde{\kappa}\, n\sigma v, \tag{6}$$

with evaporation rate $\Gamma_{\text{ev.}} = e^{-\eta} V_{\text{ev.}}/V_e$, where $\tilde{\kappa} = (\eta + 1 - X_{\text{ev.}}/V_{\text{ev.}})$ and volumes $V_{\text{ev.}}$, $X_{\text{ev.}}$, V_e are given in Appendix A. The elastic cross section is given by $\sigma = 8\pi a^2$, and the average speed by $v = \sqrt{8 k_B T/\pi m}$.

Spilling also occurs as the cutoff energy is progressively changed. This mechanism induces losses (see Appendix B)

$$\dot{N}_{\text{spl.}}/N = \tilde{\xi}\, \frac{\dot{T}}{T}, \tag{7}$$

where $\tilde{\xi} = e^{-\eta}\rho(\epsilon_c)\epsilon_c/\xi$, and an energy change

$$\dot{E}_{\text{spl.}}/E = \frac{\eta\tilde{\xi}}{\tilde{c}}\, \frac{\dot{T}}{T}. \tag{8}$$

High-energy collisions with the residual background gas lead to the atom number reduction

$$\dot{N}_{\text{loss}}/N = -\Gamma_{\text{loss}}, \tag{9}$$

with one-body loss rate, Γ_{loss}, and to an energy change

$$\dot{E}_{\text{loss}}/E = -\Gamma_{\text{loss}}, \tag{10}$$

without heating.

Finally, we also take into account the residual heating associated with incoherent light scattering processes induced by the laser beam, which increases the total energy

$$\dot{E}_{\text{heat.}}/E = (Q/\tilde{c}\, k_B T), \tag{11}$$

where $Q = 2U_0\, \omega_{\text{rec}}\, \text{Im}[\alpha]/\,\text{Re}[\alpha]$, U_0 the potential depth, α the polarizability, and $\hbar\omega_{\text{rec}}$ the recoil energy. We assume a constant value of Q and neglect particle losses resulting from this process.

Efficient evaporation is characterized by an increasing elastic collision rate, $\Gamma_{\text{el.}} = n\sigma v$, which accelerates the sample's thermalization, leading to runaway evaporation. Combining Eqs. (1)–(3) with Eqs. (5)–(11), we express the density and velocity time evolution,

$$\frac{\dot{n}}{n} = \frac{\dot{N}}{N} - \tilde{c}_2 \frac{\dot{T}}{T} = -\Gamma_{\text{loss}} + \Gamma_{\text{ev.}}\, n v \sigma \left[\frac{(\tilde{c}_2 - \tilde{\xi})(\tilde{\kappa} - \tilde{c})}{\tilde{c} - \tilde{\xi}(\eta - \tilde{c})} - 1\right] + \frac{Q}{k_B T} \frac{\tilde{\xi} - \tilde{c}_2}{\tilde{c} - \tilde{\xi}(\eta - \tilde{c})}$$

$$\frac{\dot{v}}{v} = \frac{1}{2}\frac{\dot{T}}{T} = -\frac{\Gamma_{\text{ev.}}}{2}\, n v \sigma\, \frac{\tilde{\kappa} - \tilde{c}}{\tilde{c} - \tilde{\xi}(\eta - \tilde{c})} + \frac{Q}{k_B T} \frac{1}{\tilde{c} - \tilde{\xi}(\eta - \tilde{c})},$$

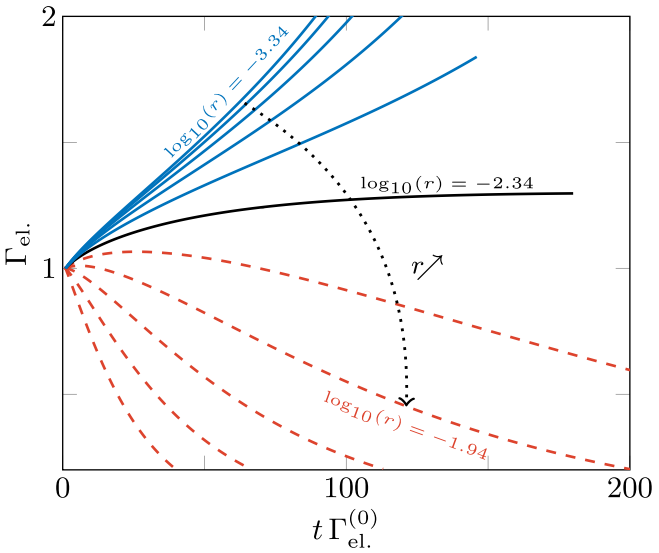

FIG. 2. Evolution of the normalized elastic collision rate for $\tilde{U}_0 = 1.25$, $\eta = 5.8$, and $s = 10^{-7}$, where $\tilde{U}_0 = U_0/\epsilon_c(t=0)$, s characterizes heating due to spontaneous emission and r one-body losses. The light blue curves correspond to values of r for which the elastic collision rate increases monotonically with time until a gain of three decades is reached in phase-space density. For values of $r > 10^{-2.34}$ this is no longer the case (red dashed). The black (straight) line represents the elastic collision rate evolution for the limiting case.

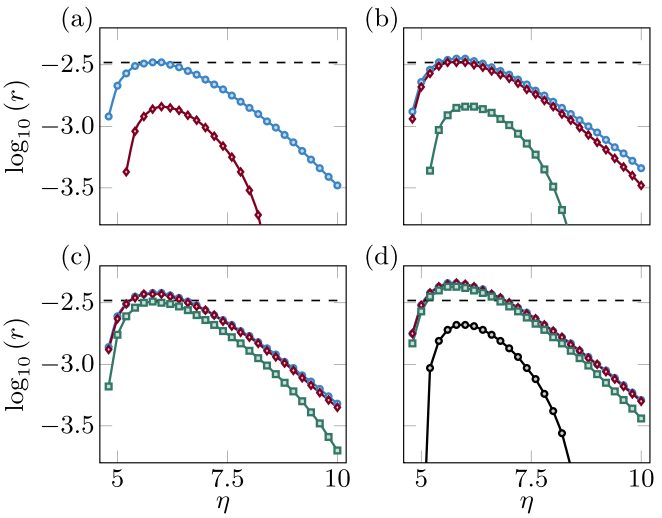

FIG. 3. Maximum value of r as a function of η for (a) $\tilde{U}_0 = 100$, (b) 10, (c) 2.5, and (d) 1.25. The different lines correspond to values of $s = 10^{-7.5}$ (light blue circles), $s = 10^{-6.5}$ (red diamonds), $s = 10^{-5.5}$ (green squares), and $s = 10^{-4.5}$ (black circles). The dashed line corresponds to the harmonic trap result $r = 0.0033$, for $s = 0$. The lines are a guide for the eye.

with $\tilde{c}_2 = \tilde{c} + \tilde{\xi} - 3/2$. These expressions can be simplified by normalizing the density and averaged speed by their respective values at $t = 0$, $n \to n/n_0$, and $v \to v/v_0$. The time is normalized by the initial collision timescale, $t \to t\,\Gamma^{(0)}_{\rm el.}$ where $\Gamma^{(0)}_{\rm el.} = n_0\sigma v_0$. The coupled equations are then given by

$$\dot{n}/n = -r + A(\eta,\, v)\, nv - \tilde{U}_0 B(\eta,\, v)\,\frac{s}{v^2} \tag{12}$$

$$\dot{v}/v = -C(\eta,\, v)\, nv + \tilde{U}_0 D(\eta,\, v)\,\frac{s}{v^2}, \tag{13}$$

with $\tilde{U}_0 = U_0/\epsilon_{\rm c}\,(t=0)$, and $A(\eta, v)$, $B(\eta, v)$, $C(\eta, v)$, $D(\eta, v)$ dimensionless, positive, functions, which tend to a constant value when $v \to 0$ (see Appendix C). The dimensionless quantities $r = \Gamma_{\rm loss}/\Gamma^{(0)}_{\rm el.}$ and $s = \frac{{\rm Im}[\alpha]}{{\rm Re}[\alpha]}(\omega_{\rm rec}/\Gamma^{(0)}_{\rm el.})$ relate to experimental limitations. In detail, r characterizes one-body losses, and s heating due to spontaneous emission. A larger s means a larger heating and a larger r more losses.

From the coupled equations Eqs. (12)–(13), one can now estimate if the finite values of r and s hinder an efficient evaporation. Since the heating rate associated with incoherent light scattering processes gains relevance as the temperature drops, the initial evolution of the elastic collision rate is not sufficient to identify the limiting experimental parameters. Therefore, we evolve the coupled equations until the phase-space density increases by three decades in logarithmic scale. As an example, we show in Fig. 2, the time evolution of the normalized elastic collision rate, $\Gamma_{\rm el.} = nv$, for $\tilde{U}_0 = 1.25$, $\eta = 5.8$, $s = 10^{-7}$, and different loss rate values. For $r < 10^{-2.34}$ the elastic collision rate increases monotonically with time resulting in a faster evaporation. This is clear from the fact that the same gain in phase-space density is reached earlier for smaller values of r. For $r \approx 10^{-2.34}$ the elastic collision rate reaches a plateau as the phase-space density approaches its final value. We define this maximum value of r as a threshold above which accelerated evaporation is impossible. However, this maximum does not imply a diverging elastic collision rate.

The same analysis is performed for different values of $\tilde{U}_0$, s, and η as shown in Fig. 3. In the absence of incoherent photon scattering processes ($s \to 0$) and an infinitely deep trap ($\tilde{U}_0 \to \infty$), we recover the well-known result $r = 0.0033$ [5],[1] as the cloud only explores the harmonic part of the dipole trap. In that limit, runaway evaporation is hindered as spontaneous emission becomes non-negligible, typically for $s \gtrsim 10^{-6}$ [see Fig. 3(a)]. From an experimental point of view, a small value of $\tilde{U}_0$ is preferable, i.e., an initial cutoff energy approximately equal to the trap depth [see Fig. 3(d)]. In that case, the one-body loss rate condition is not too stringent for $s \lesssim 10^{-4}$. Intuitively, this could be expected from Eqs. (12)–(13), but the dependence of $B(\eta,\, v)$, and $D(\eta,\, v)$ on the initial cutoff energy makes this assumption *a priori* not obvious. With that in mind, and since r and s are imposed by the initial experimental conditions, the values of η leading to an efficient evaporation can be extracted from the results shown in Fig. 3.

IV. SPECIFIC EXAMPLE FOR ^{162}Dy

To demonstrate the relevance of the cooling protocol, we consider the specific example of ^{162}Dy (nuclear spin $I = 0$), with atoms trapped in a circular polarized (σ^-) laser beam, blue detuned from the $J' = J$ optical transition with wavelength $\lambda_1 \approx 832\,$nm. For $\delta \approx 2\pi \times 40\,$GHz the two lowest-energy states $|d\rangle = |J, -J\rangle$ and $|b\rangle = |J,$

[1]See also C. Cohen-Tannoudji lectures at Collège de France, December, 3, 1996.

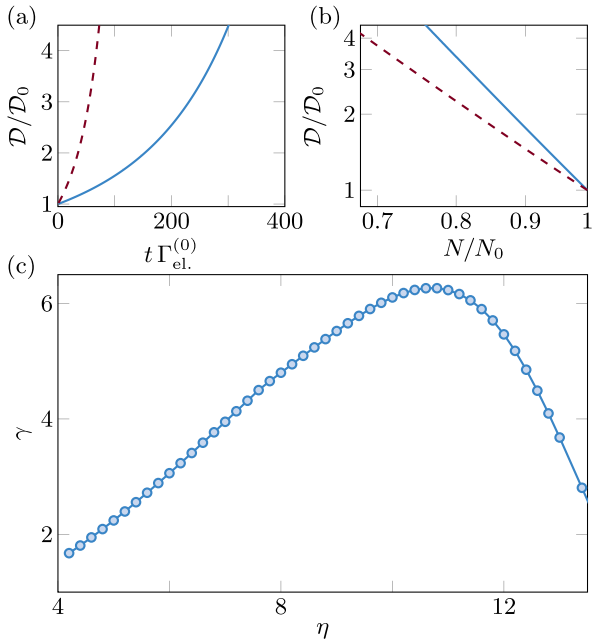

FIG. 4. Results of RF evaporation in a single optical dipole trap. (a) Gain in phase-space density as a function of time for $\eta = 7$ (red dashed line) and $\eta = 9$ (light-blue straight line). (b) Logarithmic plot of the phase-space density as a function of the total atom number for $\eta = 7$ (red dashed line) and $\eta = 9$ (light-blue straight line), resulting in $\gamma \approx 3.95$, and 5.52, respectively. (c) Initial evaporation efficiency γ, as a function of η. The line is a guide for the eye.

$-J+1\rangle$ have opposite polarizabilities $\alpha_d = -\alpha_b = 190.4\,\alpha_0$, with $\alpha_0 = 4\pi\epsilon_0 a_0^3$ and a_0 the Bohr radius [28]. The other internal states feel a strong nonlinear Zeeman shift induced by the laser beam and are not coupled by radio frequency. The ratio of real and imaginary parts of the polarizability for the two states are $(\mathrm{Re}[\alpha_d]/\,\mathrm{Im}[\alpha_d]) \approx 2.8 \times 10^7$ and $(\mathrm{Re}[\alpha_b]/\,\mathrm{Im}[\alpha_b]) \approx -3.2 \times 10^6 \sim -\delta/\Gamma$, which ensures that repumping from state $|b\rangle$ to $|d\rangle$ is negligible over the time needed for atoms in $|b\rangle$ to leave the spatial extend of the laser beam.

We consider a spin-polarized atomic ensemble with initial temperature $T(t=0) = 30\,\mu$K, and initial density $n_0 = 10^{13}\,\mathrm{cm}^{-3}$, resulting in $\Gamma_{\text{el.}}^{(0)} = 750\,\mathrm{s}^{-1}$, $s = 5.3 \times 10^{-7}$ and initial phase-space density $\mathcal{D}_0 = n\lambda^3 = 1.6 \times 10^{-4}$. Furthermore, we assume a one-body loss rate $\Gamma_{\text{loss}} = 1/60\,\mathrm{s}^{-1}$, corresponding to $r = 2.2 \times 10^{-5}$, and consider the case $\tilde{U}_0 = 1.25$.

In Figs. 4(a)–4(b), we show the gain in phase-space density for $\eta = 9$ (blue) and $\eta = 7$ (red). A standard way to optimize the evaporation efficiency is obtained by maximizing the initial gain in phase-space density per particle loss, corresponding to a large value of $\gamma = -d\log_{10}(\mathcal{D})\,/\,d\log_{10}(N)\,|_{t\to 0}$ In Fig. 4(c), we show the evolution of γ as a function of η, which peaks at $\gamma \approx 6$ for $\eta \approx 10.8$. This result suggests that heating due to incoherent photon scattering processes is negligible and efficient evaporation in deep optical dipole traps is possible. In that case, the critical phase-space density $\mathcal{D}_c \approx 2.6$ is reached over a time $t = 4.8\,\mathrm{s}$ with a final atom number $\approx 1/4$ its initial value. One can contrast this result to another example, for instance $\eta = 6$, for which runaway evaporation also occurs. In that case, degeneracy is reached after solely $\approx 0.2\,\mathrm{s}$, with 4% of the initial atom number. The choice of η is therefore setup dependent as it depends on the scientific goal and the initial experimental conditions. It is important to stress that these values are merely indicative, as the truncated Boltzmann distribution approximation is not applicable near quantum degeneracy [3].

V. DISCUSSION AND CONCLUSION

One should note that as the elastic collision rate increases, so does the density and therefore three-body losses are enhanced. We have not considered such effect as it depends on the s-wave scattering length of the species under consideration. A related discussion of that effect can be found in Ref. [18]. For ^{162}Dy with $a \approx 130\,a_0$, we do not expect these processes to be dominant.

In conclusion, the radio-frequency evaporation technique in an optical dipole trap, here reported, constitutes a viable path towards efficient evaporative cooling in experiments involving atomic species where a relatively narrow optical transition is available and for which the ground-state manifold has a nonzero total spin. After a general presentation of the method, we considered the specific example of dysprosium in an optical dipole trap with wavelength $\lambda_L \approx 832\,\mathrm{nm}$. We have shown that this technique is promising to reach quantum degeneracy in a minimalist experimental setup. Compared to standard evaporation techniques, our method benefits from runaway evaporation, which is usually unreachable for a single beam optical dipole trap.

ACKNOWLEDGMENTS

We thank Jean Dalibard for inspiring discussions and critical reading of the manuscript, and Rémy Vatré for comments on the manuscript. This work was supported by Grant No. ANR-20-CE30-0024.

APPENDIX A: DESCRIPTION OF THE EVAPORATION MECHANISM

We here summarize the derivation of the rate equations, Eqs. (1)–(11), starting from the kinetic Boltzmann equation. This derivation was originally described in Ref. [3].

1. Truncated Boltzmann distribution

We start from the Boltzmann kinetic equation

$$\left(\frac{\partial}{\partial t} + \frac{\vec{p}}{m}.\vec{\nabla}_{\vec{r}} - \vec{\nabla}_{\vec{r}}U.\vec{\nabla}_{\vec{p}}\right) f(\vec{r},\,\vec{p}) = I(\vec{r},\,\vec{p}) \tag{A1}$$

where the left-hand side is the hydrodynamic derivative of the phase-space distribution function $f(\vec{r},\vec{p})$, and the right-hand side the collision integral, which describes the speed at which $f(\vec{r},\vec{p})$ changes after an elastic collision

$$I(\vec{r},\,\vec{p}_4) = \frac{\sigma}{(2\pi\hbar)^3 m}\iint d^3p_3\,d\Omega' q \times [f(\vec{r},\,\vec{p}_1)f(\vec{r},\,\vec{p}_2) - f(\vec{r},\,\vec{p}_3)f(\vec{r},\,\vec{p}_4)], \tag{A2}$$

where $\vec{p}_3$ and $\vec{p}_4$ correspond to the momenta of the two particles before the collision, and $\vec{p}_1$ and $\vec{p}_2$ the momenta after the

collision, $\sigma = 8\pi a^2$, m the atomic mass, $\hbar$ the Planck constant and a the scattering length. We write $\vec{P} = \vec{p}_1 + \vec{p}_2 = \vec{p}_3 + \vec{p}_4$, $\vec{q}' = \frac{\vec{p}_1 - \vec{p}_2}{2}$, $\vec{q} = \frac{\vec{p}_3 - \vec{p}_4}{2}$, and define u (u') as the cosine of the angle between $\vec{P}$ and $\vec{q}$ ($\vec{q}'$), and Ω' the solid angle defined by the orientation of $\vec{q}'$ with respect to $\vec{q}$.

We assume that the system is sufficiently ergodic, i.e., that the distribution function $f(\vec{r},\ \vec{p})$ has the same value, $f(\epsilon)$, for all positions $\vec{r}$ verifying $\mathcal{H}(\vec{r},\ \vec{p}) = \frac{\vec{p}^2}{2m} + U(\vec{r}) = \epsilon$. The hydrodynamic derivative then reduces to a partial derivative over time,

$$\frac{\partial}{\partial t} f(\vec{r},\ \vec{p}) = I_{\text{out}}(\vec{r},\ \vec{p}) - I_{\text{in}}(\vec{r},\ \vec{p}), \tag{A3}$$

with I_{in} and I_{out} the input and output contributions to the collision integral, respectively. We replace $\vec{p}$ by $\vec{p}_4$, multiply Eq. (A3) by $\frac{1}{(2\pi\hbar)^3}(\mathcal{H}(\vec{r},\ \vec{p}_4) - \epsilon_e)$, such that ϵ_e is linked to $\vec{p}_4$, and integrate over $\vec{r}$ and $\vec{p}$. Using the relations $f(\mathcal{H}_i) = \int d\epsilon_i\, \delta(\mathcal{H}_i - \epsilon_i) f(\epsilon_i)$, and $\rho(\epsilon) = \frac{1}{(2\pi\hbar)^3}\iint d^3r\, d^3p\, \delta(\epsilon - \mathcal{H}(\vec{r},\ \vec{p}))$, where $\mathcal{H}_i = \mathcal{H}(\vec{r},\ \vec{p}_i)$, we get

$$\begin{aligned}\rho(\epsilon_e)\dot{f}(\epsilon_e) &= \frac{\sigma}{(2\pi\hbar)^6 m}\int d\epsilon_a\, d\epsilon_b\, d\epsilon_d [f(\epsilon_a) f(\epsilon_b) \\ &\quad - f(\epsilon_d) f(\epsilon_e)] \times \int d^3r\, d^3p_4\, d^3p_3\, d\Omega' q\ \delta(\mathcal{H}_1 - \epsilon_a) \\ &\quad \times \delta(\mathcal{H}_2 - \epsilon_b)\delta(\mathcal{H}_3 - \epsilon_d)\delta(\mathcal{H}_4 - \epsilon_e).\end{aligned} \tag{A4}$$

The first part of the right-hand side of the integral depends on the properties of the system and the second part accounts for the properties of the trap.

Using the relations

$$\begin{aligned}\mathcal{H}_1 - \epsilon_a &= U(\vec{r}) + \frac{P^2}{8m} + \frac{q^2}{2m} + \frac{Pqu'}{2m} - \epsilon_a \\ \mathcal{H}_2 - \epsilon_b &= U(\vec{r}) + \frac{P^2}{8m} + \frac{q^2}{2m} - \frac{Pqu'}{2m} - \epsilon_b \\ \mathcal{H}_3 - \epsilon_d &= U(\vec{r}) + \frac{P^2}{8m} + \frac{q^2}{2m} + \frac{Pqu}{2m} - \epsilon_d \\ \mathcal{H}_4 - \epsilon_e &= U(\vec{r}) + \frac{P^2}{8m} + \frac{q^2}{2m} - \frac{Pqu}{2m} - \epsilon_e,\end{aligned}$$

$\delta(ax) = \frac{1}{|a|}\delta(x)$, $\int dx\, \delta(x - x_1)\delta(x - x_2) = \delta(x_1 - x_2)$, and $dq^2 = 2qdq$, we get

$$\begin{aligned}\rho(\epsilon_e)\dot{f}(\epsilon_e) = \frac{\sigma}{(2\pi\hbar)^6 m}\int d\epsilon_a d\epsilon_b d\epsilon_c [f(\epsilon_a) f(\epsilon_b) - f(\epsilon_d) f(\epsilon_e)] \\ \times 2(2\pi)^3 m^3 \int d^3r\, dP\, \delta(\epsilon_a + \epsilon_b - \epsilon_d - \epsilon_e).\end{aligned} \tag{A5}$$

The integral of Eq. (A4) is non-zero only if the arguments of the Dirac functions can be equal to zero, which imposes $U(\vec{r}) < \epsilon_{\min}$ such that the integral over $\vec{r}$ reduces to $\int_{U(\vec{r})<\epsilon_{\min}} d^3\vec{r}$. Without loss of generality we assume $p_a = \min(p_a,\ p_b,\ p_d,\ p_e)$, such that $p_a + p_b < p_d + p_e$ and $p_b - p_a > p_e - p_d$, where $p_e > p_d$. The integral over P is thus limited to the domain $[p_b - p_a,\ p_a + p_b]$ with $p_a = p_{\min} = \sqrt{2m(\epsilon_{\min} - U(r))}$. These intermediate results allow us to rewrite Eq. (A4) as

$$\begin{aligned}\rho(\epsilon_e)\dot{f}(\epsilon_e) &= \frac{4(2\pi)^3 m^2}{(2\pi\hbar)^6}\sigma \int d\epsilon_a d\epsilon_b d\epsilon_d [f(\epsilon_a) f(\epsilon_b) - f(\epsilon_d) f(\epsilon_e)] \int_{U(r)\leqslant\epsilon_{\min}} dr^3 \sqrt{2m(\epsilon_{\min} - U(r))}\, \delta(\epsilon_a + \epsilon_b - \epsilon_d - \epsilon_e) \\ &= \frac{8\pi m}{(2\pi\hbar)^3}\sigma \int d\epsilon_a d\epsilon_b d\epsilon_d [f(\epsilon_a) f(\epsilon_b) - f(\epsilon_d) f(\epsilon_e)] \rho(\epsilon_{\min})\, \delta(\epsilon_a + \epsilon_b - \epsilon_d - \epsilon_e),\end{aligned} \tag{A6}$$

where $\rho(\epsilon_{\min}) = \frac{2\pi(2m)^{3/2}}{(2\pi\hbar)^3}\int_{U(r)\leqslant\epsilon_{\min}} d^3r \sqrt{\epsilon_{\min} - U(r)}$.

The authors of Ref. [3] numerically solved the Boltzmann kinetic equation with the boundary condition $f(\epsilon) = 0$ for $\epsilon > \epsilon_c$, where ϵ_c is the cutoff energy. It was shown that $f(\epsilon)$ is accurately described by a Boltzmann distribution truncated at the depth of the trap

$$f(\epsilon) \approx n\lambda^3 e^{-\epsilon/k_{\text{B}}T}\Theta(\epsilon_c - \epsilon), \tag{A7}$$

where $\Theta(x)$ is the Heaviside step function, λ the thermal de-Broglie wavelength and $n = n(\vec{0})/(\text{Erf}(\sqrt{\eta}) - 2\sqrt{\eta/\pi}e^{-\eta})$ is a density that tends towards the peak density for $\eta = \epsilon_c/k_{\text{B}}T \to \infty$. We also assume, which is verified in the main text, that the elastic collision rate dominates over the evaporation rate. This implies that the system is always in a quasiequilibrium state with an effective temperature T. The atom number is given by

$$N = \int_0^\infty d\epsilon \rho(\epsilon) f(\epsilon) = n\lambda^3 \xi(\epsilon), \tag{A8}$$

with $\xi(\epsilon_c) = \int_0^{\epsilon_c} d\epsilon \rho(\epsilon) e^{-\epsilon/k_{\text{B}}T}$ the partition function accounting for the truncation at ϵ_c. For mathematical convenience we define an effective volume V_{e} such that $V_{\text{e}} = N/n = \lambda^3\xi(\epsilon_c)$. The internal energy is given by

$$E = \int_0^\infty d\epsilon\, \epsilon f(\epsilon)\rho(\epsilon) = n\lambda^3 k_{\text{B}} T^2 \frac{d\xi(\epsilon)}{dT} = N k_{\text{B}} T \tilde{c}, \tag{A9}$$

where $\tilde{c} = d\ln\xi/d\ln T$. We note that for a constant η and in the case of power-law traps $dE/dT = E/T$. We also verify that for optical dipole traps $dE/dT \approx E/T$ for large values of η as those considered in the main text.

2. Atom number and energy variation due to evaporation

Using Eq. (A6), with $\epsilon_a \to \epsilon_1, \epsilon_b \to \epsilon_2, \epsilon_d \to \epsilon_3, \epsilon_e \to \epsilon_4$, and $\epsilon_4 > \epsilon_c$, such that $f(\epsilon_4) = 0$ and $\epsilon_3 = \epsilon_{\min}$, the number of

particles lost due to evaporation is given by

$$\begin{aligned}\dot{N}_{\text{ev.}} &= -\int_{\epsilon_4}^{\infty} d\epsilon_4 \rho(\epsilon_4)\dot{f}(\epsilon_4)\\ &= -\frac{8\pi m\sigma}{(2\pi\hbar)^3}\int_{\epsilon_c}^{\infty} d\epsilon_4 \int_0^{\epsilon_c} d\epsilon_3 \int_{\epsilon_3}^{\epsilon_c} d\epsilon_2\\ &\quad\times \int_{\epsilon_c+\epsilon_3-\epsilon_2}^{\epsilon_c} d\epsilon_1 \delta(\epsilon_1+\epsilon_2-\epsilon_3-\epsilon_4)\,\rho(\epsilon_3) f(\epsilon_1) f(\epsilon_2)\\ &= -\frac{8\pi m\sigma}{(2\pi\hbar)^3} k_{\text{B}} T (n\lambda^3)^2 e^{-\eta}\int_0^{\epsilon_c} d\epsilon\, \rho(\epsilon)[(\epsilon_c-\epsilon-k_{\text{B}}T)\\ &\quad\times e^{-\epsilon/k_{\text{B}}T} + k_{\text{B}}T e^{-\eta}] \qquad \text{(A10)}\end{aligned}$$

which simplifies into $\dot{N}_{\text{ev.}} = -n^2\sigma v e^{-\eta} V_{\text{ev.}}$ where $V_{\text{ev.}}$ is an effective volume of evaporation

$$V_{\text{ev.}} = \frac{\lambda^3}{k_{\text{B}}T}\int_0^{\epsilon_c} d\epsilon\,\rho(\epsilon)\left[(\epsilon_c-\epsilon-k_{\text{B}}T)e^{-\frac{\epsilon}{k_{\text{B}}T}} + k_{\text{B}}T e^{-\eta}\right], \quad \text{(A11)}$$

and $v = \sqrt{8k_{\text{B}}T/\pi m}$ is the average speed. The corresponding energy reduction is given by

$$\begin{aligned}\dot{E}_{\text{ev.}} &= -\int_{\epsilon_c}^{\infty} d\epsilon_4 \epsilon_4 \rho(\epsilon_4)\dot{f}(\epsilon_4)\\ &= \dot{N}_{\text{ev.}}\left[\epsilon_c + \left(1-\frac{X_{\text{ev.}}}{V_{\text{ev.}}}\right)k_{\text{B}}T\right], \qquad \text{(A12)}\end{aligned}$$

with $X_{\text{ev.}} = \frac{\lambda^3}{k_{\text{B}}T}\int_0^{\epsilon_c} d\epsilon\,\rho(\epsilon)[k_{\text{B}}T(e^{-\frac{\epsilon}{k_{\text{B}}T}} - e^{-\eta}) - (\epsilon_{\text{c}}-\epsilon)e^{-\eta}]$.

APPENDIX B: SPILLING MECHANISM

For efficient evaporation, the cutoff energy is progressively decreased at a rate $1/\tau = -\dot{\epsilon}_c/\epsilon > 0$, leading to particle loss

$$\dot{N}_{\text{spl.}} = -\frac{1}{\tau}N(\epsilon_c), \qquad \text{(B1)}$$

where $N(\epsilon_c) = \rho(\epsilon_c)f(\epsilon_c)\epsilon_c$. For a constant $\eta = \epsilon_c/k_{\text{B}}T$ and $f(\epsilon_c) = \frac{N}{V_{\text{e}}}\lambda^3 e^{-\eta}$, we get that

$$\dot{N}_{\text{spl.}}/N = \eta\, k_{\text{B}}\dot{T}\,\frac{\lambda^3 e^{-\eta}\rho(\epsilon_c)}{V_{\text{e}}} = \tilde{\xi}\frac{\dot{T}}{T}, \qquad \text{(B2)}$$

where

$$\tilde{\xi} = \frac{\lambda^3 e^{-\eta}\rho(\epsilon_c)}{V_{\text{e}}}\eta k_{\text{B}}T = \frac{e^{-\eta}\rho(\epsilon_c)}{\xi}\epsilon_c. \qquad \text{(B3)}$$

Accordingly, the energy change is given by

$$\dot{E}_{\text{spl.}} = \epsilon_c\dot{N}_{\text{spl.}} = \frac{\tilde{\xi}\eta}{\tilde{c}}\frac{\dot{T}}{T}E, \qquad \text{(B4)}$$

where $E = Nk_{\text{B}}T\tilde{c}$.

APPENDIX C: DETAILED DESCRIPTION OF EQS. (12)–(13)

We here give the detailed expressions for the dimensionless functions $A(\eta,\ v)$, $B(\eta,\ v)$, $C(\eta,\ v)$, and $D(\eta,\ v)$ introduced in Eqs. (12)–(13)

$$\begin{aligned}A(\eta,\ v) &= \Gamma_{\text{ev.}}\left[\frac{(\tilde{c}_2-\tilde{\xi})(\tilde{\kappa}-\tilde{c})}{\tilde{c}-\tilde{\xi}(\eta-\tilde{c})} - 1\right]\\ B(\eta,\ v) &= 2\eta\frac{\tilde{c}_2-\tilde{\xi}}{\tilde{c}-\tilde{\xi}(\eta-\tilde{c})}\\ C(\eta,\ v) &= \frac{\Gamma_{\text{ev.}}}{2}\frac{\tilde{\kappa}-\tilde{c}}{\tilde{c}-\tilde{\xi}(\eta-\tilde{c})}\\ D(\eta,\ v) &= \eta\frac{1}{\tilde{c}-\tilde{\xi}(\eta-\tilde{c})},\end{aligned}$$

where $\tilde{\kappa}$, $\tilde{\xi}$, $\tilde{c}$, $\tilde{c}_2$, and $\Gamma_{\text{ev.}}$ are functions of η and v. For $v \to 0$ and a constant, finite η, these expressions tend to the solutions of a harmonic trap. Namely, $\Gamma_{\text{ev.}} = e^{-\eta}[\eta - 4R(3,\eta)]$, $\tilde{\kappa} = \eta + 1 - \frac{P(5,\eta)}{P(3,\eta)}\frac{e^{-\eta}}{\Gamma_{\text{ev.}}}$, $\tilde{\xi} = 3[1-R(3,\eta)]$, $\tilde{c} = 3R(3,\eta)$. and $\tilde{c}_2 = 3/2$, where $P(a,z)$ is the incomplete Γ function, and $R(a,z) = P(a+1,z)/P(a,z)$ [5].

[1] M. H. Anderson, J. R. Ensher, M. R. Matthews, C. E. Wieman, and E. A. Cornell, Science **269**, 198 (1995).

[2] H. F. Hess, Phys. Rev. B **34**, 3476 (1986).

[3] O. J. Luiten, M. W. Reynolds, and J. T. M. Walraven, Phys. Rev. A **53**, 381 (1996).

[4] W. Ketterle and N. J. V. Druten, *Advances In Atomic, Molecular, and Optical Physics* (Academic Press, New York, 1996), Vol. 37, pp. 181–236.

[5] D. Guéry-Odelin, Dynamique collisionnelle des gaz d'alcalins lourds : du refroidissement évaporatif à la condensation de Bose-Einstein, Université Pierre et Marie Curie, 1998, https://tel.archives-ouvertes.fr/tel-00001134/file/tel-00001134.pdf.

[6] C. S. Adams and E. Riis, Prog. Quantum Electron. **21**, 1 (1997).

[7] M. Inguscio, S. Stringari, and C. Wieman, *Bose-Einstein Condensation in Atomic Gases*, Vol. 140 (IOS Press, Amsterdam, 1999).

[8] W. Ketterle, Rev. Mod. Phys. **74**, 1131 (2002).

[9] E. A. Cornell and C. E. Wieman, Rev. Mod. Phys. **74**, 875 (2002).

[10] Y. Colombe, E. Knyazchyan, O. Morizot, B. Mercier, V. Lorent, and H. Perrin, Europhys. Lett. **67**, 593 (2004).

[11] R. Grimm, M. Weidemüller, and Y. B. Ovchinnikov, *Advances In Atomic, Molecular, and Optical Physics* (Academic Press, New York, 2000), Vol. 42, pp. 95–170.

[12] M. D. Barrett, J. A. Sauer, and M. S. Chapman, Phys. Rev. Lett. **87**, 010404 (2001).

[13] S. R. Granade, M. E. Gehm, K. M. O'Hara, and J. E. Thomas, Phys. Rev. Lett. **88**, 120405 (2002).

[14] Y. Takasu, K. Maki, K. Komori, T. Takano, K. Honda, M. Kumakura, T. Yabuzaki, and Y. Takahashi, Phys. Rev. Lett. **91**, 040404 (2003).

[15] T. Weber, J. Herbig, M. Mark, H.-C. Nägerl, and R. Grimm, Science **299**, 232 (2003).

[16] T. Fukuhara, Y. Takasu, M. Kumakura, and Y. Takahashi, Phys. Rev. Lett. **98**, 030401 (2007).
[17] K. M. O'Hara, M. E. Gehm, S. R. Granade, and J. E. Thomas, Phys. Rev. A **64**, 051403(R) (2001).
[18] D. Wilkowski, J. Phys. B: At., Mol. Opt. Phys. **43**, 205306 (2010).
[19] T. Kinoshita, T. Wenger, and D. S. Weiss, Phys. Rev. A **71**, 011602(R) (2005).
[20] J.-F. Clément, J.-P. Brantut, M. Robert-de Saint-Vincent, R. A. Nyman, A. Aspect, T. Bourdel, and P. Bouyer, Phys. Rev. A **79**, 061406(R) (2009).
[21] A. B. Deb, T. McKellar, and N. Kjærgaard, Phys. Rev. A **90**, 051401(R) (2014).
[22] C. Chin, R. Grimm, P. Julienne, and E. Tiesinga, Rev. Mod. Phys. **82**, 1225 (2010).
[23] A. L. Gaunt, T. F. Schmidutz, I. Gotlibovych, R. P. Smith, and Z. Hadzibabic, Phys. Rev. Lett. **110**, 200406 (2013).
[24] J. H. Becher, S. Baier, K. Aikawa, M. Lepers, J.-F. Wyart, O. Dulieu, and F. Ferlaino, Phys. Rev. A **97**, 012509 (2018).
[25] S. Stellmer, F. Schreck, and T. C. Killian, in *Annual Review of Cold Atoms and Molecules*, Annual Review of Cold Atoms and Molecules, Vol. 2 (World Scientific, Singapore, 2013), pp. 1–80.
[26] S. Eustice, K. Cassella, and D. Stamper-Kurn, Phys. Rev. A **102**, 053327 (2020).
[27] M. Yan, R. Chakraborty, A. Mazurenko, P. G. Mickelson, Y. N. M. de Escobar, B. J. DeSalvo, and T. C. Killian, Phys. Rev. A **83**, 032705 (2011).
[28] W. Kao, Y. Tang, N. Q. Burdick, and B. L. Lev, Opt. Express **25**, 3411 (2017).